European Journal of Pharmaceutics and Biopharmaceutics 141 (2019) 70–80

Contents lists available at ScienceDirect

European Journal of Pharmaceutics and Biopharmaceutics

journal homepage: www.elsevier.com/locate/ejpb

Research paper

Effect of nanoparticle size and PEGylation on the protein corona of PLGA nanoparticles

Katrin Partikel[a], Robin Korte[b], Nora C. Stein[a], Dennis Mulac[a], Fabian C. Herrmann[c], Hans-Ulrich Humpf[b], Klaus Langer[a,*]

[a] Institute of Pharmaceutical Technology and Biopharmacy, University of Muenster, Corrensstraße 48, 48149 Muenster, Germany
[b] Institute of Food Chemistry, University of Muenster, Corrensstraße 45, 48149 Muenster, Germany
[c] Institute of Pharmaceutical Biology and Phytochemistry, University of Muenster, Corrensstraße 48, 48149 Muenster, Germany

ARTICLE INFO

Keywords:
Nanoparticles
Poly(lactide-co-glycolic acid)
Poly(ethylene glycol)
Protein corona
Proteomics
Particle size
Stealth coatings
'Stealth' nanoparticles

ABSTRACT

Upon intravenous administration of nanoparticles (NP) into the bloodstream, proteins bind rapidly on their surface resulting in a formation of a so-called 'Protein Corona'. These proteins are strongly attached to the NP surface and provide a new biological identity which is crucial for the reaction at the nano-biointerface. The structure and composition of the protein corona is greatly determined by the physico-chemical properties of the NP and the characteristics of the biological environment. The overall objective of this study was to characterize the role of NP size/surface curvature and PEGylation on the formation of the protein corona. Therefore, we prepared NP in a size of 100 and 200 nm using the biodegradable polymers poly(DL-lactide-co-glycolide) (PLGA) and poly(DL-lactide-co-glycolide)-co-polyethylene glycol diblock (PLGA-PEG) and subsequently incubated them with fetal bovine serum (FBS) to induce the formation of a protein corona. After removal of unbound protein, we employed different analytical approaches to study the corona in detail. Sodium dodecylsulfate polyacrylamide gel electrophoresis (SDS-PAGE) was performed to gain a first impression about amount and composition of the corona proteins. Identification was carried out after tryptic in-solution digestion and liquid chromatography–mass spectrometry/mass spectrometry (LC–MS/MS). In addition, we successfully established the Bradford protein assay as a suitable colorimetric method to quantify total adsorbed protein amount after alkaline hydrolysis of PLGA based NP. Our results revealed that protein adsorption on PLGA- and PLGA-PEG-NP didn't depend on NP size within the range of 100 and 200 nm. PEGylation led to a significant reduced amount of bound proteins. The depletion of proteins which are involved in immune response was remarkable and indicated a prolonged circulation time in body.

1. Introduction

Besides the wide use of nanomaterials in industrial products, nanoparticles (NP) are increasingly considered for use in biomedical applications including imaging, diagnosis, and targeted drug delivery [1]. NP exhibit unique physicochemical properties compared to their bulk material resulting in a high surface to volume ratio and an active surface chemistry [1,2]. Immediately after administration into a biological fluid NP tend to interact with proteins in order to reduce their large surface energy [3]. Consequently, this leads to the formation of a protein corona [4]. Corona formation is a very dynamic, competitive and time dependent process. In the early stage proteins with low affinities and fast exchange rates bind to the particle surface and are later replaced by proteins with a higher affinity and lower abundance in serum, for instance apolipoproteins and immunoglobulins [4,5]. These proteins are considered as the 'hard' protein corona and provide the NP a new biological identity which could be substantially different from their pristine state and dictate the biological fate in the body in terms of biodistribution, cellular uptake, and trafficking [6]. The identity, amount, and conformational state of the bound proteins highly depend on the physicochemical properties of the NP (e.g. nanomaterial, size, shape, charge, surface functional groups, hydrophobicity) and the exposing environment including the origin of the biological fluid (e.g. bovine or human), protein concentration, exposure time, pH, temperature, and shear stress [6,7]. Understanding the correlation between NP properties, protein corona formation and its reaction at the nano-biointerface is crucial for the development of safer and more efficient NP based drug delivery systems.

* Corresponding author.
E-mail address: k.langer@uni-muenster.de (K. Langer).

https://doi.org/10.1016/j.ejpb.2019.05.006
Received 2 November 2018; Received in revised form 4 February 2019; Accepted 9 May 2019
Available online 10 May 2019
0939-6411/

Hence, the aim of the given study was to investigate the effect of NP size and surface modification with poly(ethylene glycol) (PEG) on the formation of the protein corona. Therefore, NP in a size of 100 and 200 nm using the polymers poly(DL-lactide-co-glycolide) (PLGA) and poly(DL-lactide-co-glycolide)-co-polyethylene glycol diblock with 15 wt% PEG (PLGA-PEG) were produced. PLGA is approved by the US FDA and the European Medicine Agency (EMA) for several applications because of its biodegradability, biocompatibility, and sustained release properties, thus offering outstanding opportunities for the development of controlled and targeted drug delivery systems [8]. However, opsonization leads to a recognition of nanocarriers by the cells of the mononuclear phagocyte system (MPS) and a rapid elimination from the systemic circulation [9]. A common approach to overcome this obstacle is to functionalize the surface with PEG in order to impart 'stealth' properties. PEGylation shields the NP from opsonization and phagocytosis and therefore improves their pharmacokinetic behavior [9–11].

In order to evaluate the impact of size and 'stealth' properties of the different prepared NP systems, an incubation with fetal bovine serum (FBS) was performed to induce the formation of a protein corona. FBS was used as protein source because it is a common additive in standard cell culture media for many human cell lines [12]. Moreover, it is well known that the protein adsorption is affected by the protein concentration of the incubation solution [4,13,14]. For example, when the available nanoparticle surface is in excess over the total protein concentration, the adsorption of low affinity proteins is enhanced [4]. In order to avoid these effects, we fixed the ratio of total particle surface area to serum for all experiments. After incubation and separation of NP from excess serum, we employed sodium dodecylsulfate polyacrylamide gel electrophoresis (SDS-PAGE) and liquid chromatography–mass spectrometry/mass spectrometry (LC–MS/MS) to study the corona composition in detail. Moreover, the well-established Bradford protein assay was used as a novel application for quantification of total adsorbed protein amount after alkaline hydrolysis of PLGA based NP systems.

2. Material and methods

2.1. Reagents

The biodegradable polymers poly(DL-lactide-co-glycolide) (PLGA, Resomer® RG 502 H, inherent viscosity 0.19 dL/g, M_W 12,000 g/mol, D,L-lactide (50 mol%): glycolide (50 mol%)) and poly(DL-lactide-co-glycolide)-co-polyethylene glycol diblock with 15 wt% PEG (PLGA-PEG, Resomer® Select 5050 DLG mPEG 5000, inherent viscosity 0.52 dL/g, M_W 48.3 kDa, D,L-lactide (50 mol%): glycolide (50 mol%)), which were used as NP matrices, were obtained from Evonik Industries (Darmstadt, Germany). The steric NP stabilizer poly(vinyl alcohol) (PVA, Mowiol® 8–88, molecular weight approx. 67,000 g/mol) was purchased from Merck KGaA (Darmstadt, Germany). Fetal bovine serum (FBS) superior was received from Biochrom AG (Berlin, Germany). Roti-Load®1, Roti®-Mark STANDARD, and all other chemicals used for SDS-PAGE were delivered by Carl Roth GmbH & Co. KG (Karlsruhe, Germany). Coomassie Brilliant Blue G-250 was purchased from VWR Life science AMRESCO (Solon, Ohio). Bovine serum albumin (BSA), DL-dithiothreitol (DTT), and iodoacetamide (IAA) were obtained from Sigma-Aldrich (Steinheim, Germany). Trypsin (sequencing grade) for protein digestion was obtained from Promega Corporation (Madison, USA). Urea was purchased from Acros Organics (New Jersey, USA). All other chemicals and organic solvents were delivered in the highest grade available.

2.2. Nanoparticle preparation

Several top-down synthesis techniques for NP based on the polymers PLGA and PLGA-PEG are well described in literature [15]. Here, two partially modified preparation methods for NP with a diameter of 100 and 200 nm were used [16,17].

2.2.1. Preparation of 100 nm PLGA and PLGA-PEG nanoparticles

NP with a diameter of 100 nm were manufactured by a solvent displacement method. Therefore, 30 mg PLGA was dissolved in 2 mL acetone. The organic solution was injected into 4 mL of an aqueous PVA solution (2%, m/m) under a constant stirring rate of 500 rpm. The resulting emulsion was stirred overnight at room temperature to remove the organic phase and to induce the formation of the NP. The obtained NP suspension was washed three times by centrifugation (2.5 h, 13,000*g*) and redispersion in ultrapure water. The NP were referred to as PLGA-100-NP.

For preparation of the PEGylated formulation, 130 mg PLGA-PEG was dissolved in 2 mL acetone and subsequently injected into 4 mL PVA solution (2%, m/m) under stirring at 500 rpm. After evaporation of the organic phase the purification of the suspension was performed likewise. The NP were referred to as PLGA-PEG-100-NP.

2.2.2. Preparation of 200 nm PLGA and PLGA-PEG nanoparticles

NP with a diameter of 200 nm were prepared using an emulsion diffusion method. Therefore, 100 mg PLGA was dissolved in 2 mL ethylacetate and subsequently added to 4 mL of an aqueous solution containing PVA (2%, m/m). The mixture was emulsified using a high-speed homogenizer (Ultra-Turrax®, S25NK-10G, IKA, Staufen, Germany) at 21,000 rpm for 30 min. The resulting pre-emulsion was poured into 6 mL of PVA solution (2%, m/m) and stirred overnight at room temperature to remove the organic solvent. Finally, the NP were purified by three steps of centrifugation (10 min, 16,000*g*) and subsequent resuspension in ultrapure water. The NP were referred to as PLGA-200-NP.

In order to produce PEGylated NP, 100 mg PLGA-PEG was dissolved in 4 mL ethylacetate. For emulsification the organic solution was added to 7 mL aqueous PVA solution (2%, m/m). The mixture was homogenized with the Ultra-Turrax® (S25N-19G, IKA, Staufen, Germany) at 15,000 rpm for 35 min. Afterwards, the pre-emulsion was diluted with 3 mL PVA solution (2%, m/m) and stirred overnight. Purification of the suspension was carried out as described above. The NP were referred to as PLGA-PEG-200-NP.

2.3. Nanoparticle characterization

2.3.1. Determination of particle diameter, size distribution, and zeta potential

The hydrodynamic NP diameter and polydispersity index (PDI) were detected by photon correlation spectroscopy (PCS) using a Malvern Zetasizer Nano ZS system (Malvern Instruments Ltd., Malvern, United Kingdom). An appropriate volume of the different purified NP formulations was diluted with 2 mL ultrapure water in a disposable cuvette right before use and measured at a temperature of 22 °C using a backscattering angle of 173°.

The zeta potential was measured in the same instrument by laser Doppler microelectrophoresis to provide information about the surface charge of the NP. Therefore, the NP dilutions described above were transferred into a folded capillary cell and the determination was conducted at 22 °C.

2.3.2. Nanoparticle yield

The NP yield of the different NP formulations was determined gravimetrically. Therefore, an aliquot of 20.0 µL NP suspension was transferred into a micro weighing dish and dried for at least 2 h at 80 °C until mass constancy.

2.3.3. Morphological analysis of nanoparticles by atomic force microscopy

The dimensions and the morphology of the prepared NP was investigated by atomic force microscopy (AFM) employing a Bruker Dimension 3100 atomic force microscope, equipped with a Nanoscope

IIIa controller (Bruker, Karlsruhe, Germany). Initially, 3 μL of NP suspension (0.2 mg/mL) were transferred onto a cleaned glass slide and subsequently air dried. Imaging was performed afterwards in intermittend contact mode (Tapping Mode™) with n-type silicon cantilevers (HQ:NSC14/Al BS, nominal tip radius < 10 nm, typical resonant frequency of about 160 kHz and a nominal spring constant of 5 N/m; manufactured by μmash, Sofia, Bulgaria), 2% below resonance frequency at a RMS amplitude of around 2. Further data analysis was carried out using NanoScope Analysis version 1.5.

2.4. Serum protein adsorption

Sample preparation for serum protein adsorption was carried out according to a modified method described by Gossmann et al. [3]. For all experiments the ratio of total particle surface area to serum was kept constant to ensure comparability between the obtained results and to exclude effects that attribute to other phenomenons than particle size or surface modification with PEG.

For the calculation of the total surface area of the NP suspension under the assumption of a spherical particle shape ($A = 4\pi r^2$) the density, the hydrodynamic diameter and the yield of the NP were required. The particle density was measured by a DM40 LiquiPhysics™ Excellence system (Mettler Toledo GmbH, Greifensee, Swiss). Densities of 1.354 g/cm^3 and 1.367 g/cm^3 were achieved for PLGA-100-NP and PLGA-200-NP, respectively. For both, PLGA-PEG-100-NP and PLGA-PEG-200-NP, a density of 1.347 g/cm^3 was determined.

For SDS-PAGE analysis and protein quantification by Bradford protein assay, an aliquot corresponding to 0.08 m^2 total particle surface was taken from the NP suspensions, mixed with 500 μL FBS and then filled up to a total volume of 2 mL with ultrapure water. After that, the samples were incubated for 30 min at 37 °C under shaking at 1200 rpm in a Thermomixer® comfort (Eppendorf AG, Hamburg, Germany). Finally, the samples were purified to remove excess protein. Hence, the NP were centrifuged (30 min, 30,000*g*) five times, the supernatant was discarded and the pellet was resuspended in ultrapure water. For identification of the proteins in the corona by LC–MS analysis a larger particle surface area was required. Therefore, 1000 μL FBS was added to a volume of NP suspension corresponding to 0.24 m^2 particle surface and filled up to a total volume of 4 mL with ultrapure water. The unbound protein amount was removed as already described.

2.5. SDS-PAGE analysis of corona proteins

After protein adsorption and final centrifugation step the pellet was resuspended under shaking (1200 rpm, 22 °C) in 30 μL reducing loading buffer (Roti-Load®1) overnight to desorb the proteins from the NP surface. Hereafter, the samples were centrifuged again (45 min, 30,000*g*) in order to separate the desorbed proteins from the NP. Therefore, the pellet was discarded and the supernatant was transferred into a new reaction vessel and heated for 5 min at 95 °C to denature the proteins. Subsequently, a 10% polyacrylamide gel was prepared and the samples as well as the protein standard (Roti®-Mark STANDARD), negative controls, and a positive control were applied on the gel. For negative controls, the NP were incubated with water instead of FBS. All other steps were performed identically. For positive control, FBS was diluted 1:100 with ultrapure water. The SDS-PAGE was carried out at a constant voltage of 200 V for 1 h on an OmniPAGE mini system (Omnilab-Laborzentrum GmbH & Co. KG, Bremen, Germany). The resulting gel was fixed (79% water, 1% orthophosphoric acid, 20% methanol), stained with a colloidal Coomassie Brilliant Blue G-250 solution overnight and destained in methanol:water (1:3, v/v). Finally, Gel iX Imager (INTAS Science Imaging Instruments GmbH) was used for imaging.

2.6. Quantification of corona proteins using Bradford protein assay

For the quantification of corona proteins, a photometric method based on a protein determination protocol by Bradford et al. was used [18]. The dye Coomassie Brilliant Blue G-250 binds to the proteins and causes a shift in the absorption maximum from 465 to 595 nm which can be read in a spectrophotometer.

For this assay, the previously obtained NP pellet was hydrolyzed with 100 μL NaOH 1 M and 400 μL purified water (15 min, 60 °C, 1200 rpm Eppendorf Thermomixer® comfort). Afterwards, 1.9 mL Bradford reagent was added to 100 μL of the hydrolyzed sample. Incubation for 10 min at 1200 rpm led to a stable protein–dye complex which was monitored at 595 nm using a spectrophotometer Typ U-2900 (Hitachi High Technologies Corporation, Tokyo, Japan). The NP bound protein amount was calculated using a BSA calibration curve with addition of NaOH 1 M in a range of 0.05–0.5 mg/mL.

This method was validated in terms of accuracy, precision, and linearity according to the ICH harmonized tripartite guideline "Validation of analytical procedures: Text and Methodology Q2(R1)" (2005). The validation was conducted with pure BSA and BSA plus hydrolyzed PLGA-PEG in order to exclude interferences which are caused by hydrolyzed components of PLGA-PEG and Coomassie Brilliant Blue G-250. The experiments were performed at low, middle, and high concentrations of BSA covering the specific range for the procedure. The samples were measured six fold and analyzed as described above.

2.7. Identification of corona proteins by LC–MS/MS

Corona proteins were identified using a shotgun proteomics based approach, which has become the standard technique for the investigation of complex protein mixtures in recent years. Following tryptic digestion of the proteins, peptides were identified using LC–MS/MS on an orbitrap-based mass spectrometer and software-based data evaluation to interpret the peptide fragmentation data. In this study we referred to a protocol of Gossmann et al. [3].

2.7.1. In-solution digestion of corona proteins

After washing and collecting the NP with protein corona by centrifugation as described above, the resulting pellet was resuspended in TRIS buffer containing 6 M urea overnight at room temperature to desorb the proteins from the surface. Following this, the samples were centrifuged again (45 min, 30,000*g*) in order to isolate the desorbed proteins. The supernatant consisting of corona proteins was mixed with 5 μL of 200 mM dithiothreitol for 1 h at room temperature to reduce the disulfide bonds. Subsequently, 20 μL of 200 mM iodoacetamide was added to the solution in order to alkylate cysteines. The reaction was conducted for 1 h in the dark. Excess iodoacetamide was thereafter inactivated by another addition of dithiothreitol (20 μL, 200 mM, 1 h, 1200 rpm, 22 °C). To prepare tryptic in-solution digestion of proteins, the samples were diluted to a total volume of 1000 μL with ultrapure water to a final concentration of 0.6 M urea to maintain the activity of trypsin. Next, 10 μL of ice-cold trypsin solution (200 ng/μL) was added to the diluted samples and digestion was carried out overnight under slight shaking (37 °C, 900 rpm). Finally, the reaction was stopped by adjusting the pH to < 6 with glacial acetic acid and the samples were filled up to a total volume of 2 mL with ultrapure water for the further experimental procedure.

2.7.2. Peptide purification

To prepare for a successful mass spectrometric analysis of the peptides the samples were purified by solid-phase-extraction in order to remove salts and undesired impurities. Briefly, Strata™-X 33 μm RP 30 mg/1 mL columns (Phenomenex, Aschaffenburg, Germany) were sequentially activated and equilibrated with 1 mL methanol and 1 mL 1% formic acid before the digestion solutions were applied onto the

columns in aliquots of 1 mL. Thereafter, the samples were desalted by washing with 1 mL of purified water. Then, the stationary phase including the peptides was rinsed with 600 µL of Eluent I (MeOH/H_2O + 1% FA (5:5)) followed by 400 µL of Eluent II (MeOH/H_2O + 1% FA (7:3)). The eluents were collected and evaporated nearly to dryness in a Thermomixer® comfort (40 °C, 300 rpm) under nitrogen atmosphere. Finally, the residue was redissolved in a mixture of 100 µL acetonitrile, formic acid, and purified water (3:1:96, v/v) and the samples were stored at −20 °C until LC-MS/MS analysis.

2.7.3. Mass spectrometric detection of peptides

Data were acquired on an LTQ Orbitrap XL hybrid ion trap-orbitrap mass spectrometer coupled to an Accela HPLC system (both Thermo Scientific, Dreieich, Germany). The injection volume was 20.0 µL and LC separation of enzymatic digests was carried out on an 2.1 × 150 mm, 2.6 µm Accurore C18 column (Thermo Scientific) at a constant flow rate of 250 µL/min employing the following gradient of ACN + 1% formic acid (A) and H_2O + 1% formic acid (B): 3% A for 6 min, 3–12% A in 6 min, 12–35% A in 79 min, 35–60% A in 9 min, holding 60% A for 8 min, 60–3% A in 2 min and reequilibration at 3% A in 10 min. The mass spectrometer was operated in positive full scan and data-dependent mode (DDMS). Survey full-scan mass spectra (m/z 300–1500) were acquired in the Orbitrap (resolution r = 30,000) and the two most intense ions were sequentially isolated, fragmented, and analyzed in the linear ion trap, using collision-induced dissociation (CID, normalized collision energy of 30% and an activation time of 30 ms). No charge states were rejected from fragmentation and target ions were dynamically excluded from repeated fragmentation for 45 s. Conditions for electrospray ionization (ESI) were: Capillary temperature 225 °C; vaporizer temperature 350 °C; sheath gas flow 40 (arbitrary units); auxiliary gas flow 20 (arbitrary units); sweep gas flow 5 (arbitrary units), source voltage 3.5 kV; and tube lens 135 V.

2.7.4. Data evaluation

For protein identification a database search was performed with PEAKS 7 (Bioinformatics Solutions, Waterloo, Canada) against the UniProt KB database (*Bos taurus*, created 2016-04-25, 43,803 entries) using the PEAKS *de novo* algorithm and the enhanced target-decoy method ("decoy fusion") for false discovery rate (FDR) estimation and result validation [19,20]. Search parameters were: (a) trypsin as specific enzyme, three missed cleavage allowed; (b) fixed modification: Carbamidomethylation of cysteine and variable modification: Oxidation of methionine, allowing three variable PTM per peptide; (c) precursor mass error tolerance of 5 ppm; (d) fragment mass error tolerance of 1 Da. Proteins with a -lgP value > 80 were considered to be reliable.

2.8. Statistical methods

All experiments were performed at least three times. The results were shown as average value with standard deviation. Significance tests were conducted with Sigma Plot 12.5 (Systat Software GmbH, Erkrath, Germany), using a one way ANOVA test with the Holm-Sidak post test. Significance levels were depicted as * for $p \leq 0.05$.

3. Results

3.1. Nanoparticle preparation and physicochemical characterization

NP manufactured and analyzed in the present study were based on the biodegradable polymer PLGA and sterically stabilized with PVA. In order to monitor the effect of the NP size and surface curvature on the formation of the protein corona derived from FBS, NP with a diameter of 100 and 200 nm were prepared. To assess the influence of 'stealth' properties on the protein corona formation, the surface of the PLGA-NP was functionalized with PEG. Therefore, an amphiphilic PLGA-PEG diblock copolymer with 15% wt PEG (5 kDa) was used.

Table 1
Physicochemical characteristics of the investigated nanoparticle systems (mean ± SD; n ≥ 3).

Nanoparticle system	Particle diameter [nm]	PDI	Zeta potential [mV]
PLGA-100-NP	110.6 ± 6.0	0.06 ± 0.02	−41.2 ± 8.1
PLGA-200-NP	214.6 ± 13.2	0.03 ± 0.03	−41.1 ± 5.2
PLGA-PEG-100-NP	93.8 ± 7.3	0.07 ± 0.03	−40.1 ± 4.5
PLGA-PEG-200-NP	242.5 ± 5.5	0.05 ± 0.01	−39.3 ± 3.9

The physicochemical properties of the different NP formulations were determined with regard to hydrodynamic diameter, polydispersity index, and zeta potential in a Malvern Zetasizer. As summarized in Table 1, the variation in preparation technique provided different sized NP in the desired range. All formulations showed a monodisperse size distribution with PDI values < 0.1. Both systems, irrespective of PLGA or PLGA-PEG as matrix polymer, displayed a negative surface charge of about −40 mV. Atomic force microscopy images confirmed the spherical shape of the NP and the smoothness of the surface (Fig. 1). In a previous study of our group XPS measurements were used to characterize the surface structure of these NP in more detail [16]. It could be shown that similar NP based on PLGA-PEG exhibited a surface PEG coverage of 15.1 wt% PEG in combination with 52.3 wt% PLGA and 33.6 wt% PVA whereas the surface of PLGA-NP consisted of 92.4 wt% PLGA and 7.5 wt% PVA.

3.2. Characterization of protein corona after serum protein adsorption

3.2.1. SDS-PAGE analysis

One-dimensional SDS-PAGE analysis was performed to separate the corona proteins on the basis of their molecular mass and to gain a first impression about protein composition and relative abundance. The electrophoresis was carried out in triplicate. The profiles of separated proteins were reproducible and one typical gel is shown in Fig. 2. Besides the protein corona pattern of PLGA and PLGA-PEG-NP, a positive control from diluted FBS and negative controls derived from 100 to 200 nm PLGA-PEG-NP are displayed.

The protein pattern of the positive control was dominated by one major band corresponding to the molecular weight of serum albumin (67 kDa). In contrast, PLGA-NP showed an accumulation of many serum proteins on their surface. The masses of visible polypeptides ranged from 29 to 212 kDa. A sharply defined band was located at the top of the gel between 118 and 212 kDa. The highest intensity of protein staining appeared between 43 and 118 kDa while the three protein bands above 29 kDa typically occurred in the corona of PLGA-NP. Furthermore, the composition and staining intensity of protein bands for 100 and 200 nm PLGA-NP were identical.

In comparison to the corona of PLGA-NP, the PLGA-PEG-NP yielded a protein pattern consisting of less protein bands with considerably lower intensity. The only bands visible were localized around 66 kDa and were highlighted with arrows. Again, the protein profiles were similar for the two different particle diameters. Moreover, the absence of protein bands in the negative controls proved that the samples were not contaminated with other proteins during the preparation procedure.

3.2.2. Protein quantification using Bradford assay

In order to quantify the total protein amount adsorbed onto the surface of the different NP systems and to access the impact of different particle size and PEGylation Bradford protein assay was established as a new analytical tool. The quantification was conducted after alkaline hydrolysis of the isolated NP-protein complex to minimize disturbance of the used compounds. Prior to this we examined the effect of hydrolyzed NP on the absorbance and carried out a method validation. For this purpose PLGA-PEG-NP were chosen as an appropriate model system because these NP cover all used ingredients which could be

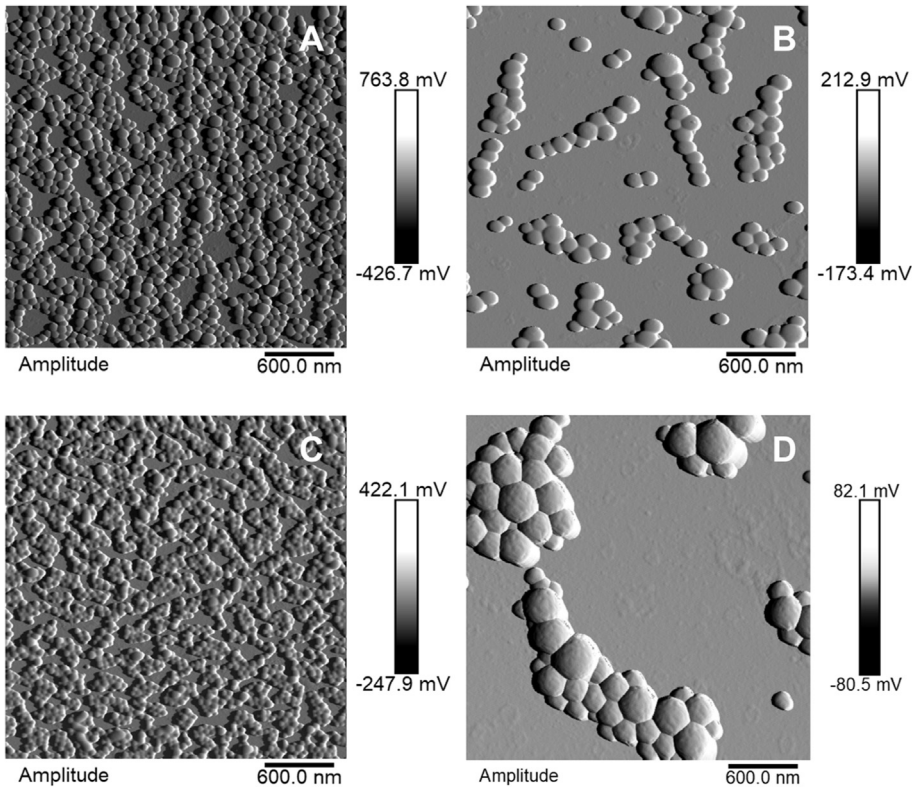

Fig. 1. Atomic force microscopy (AFM) pictures of PLGA-100-NP (A); PLGA-200-NP (B); PLGA-PEG-100-NP (C); PLGA-PEG-200-NP (D). The images confirmed the spherical shape of the NP and the smooth surface without local asperities.

relevant for interferences with the protein-dye complex.

The validation procedure was performed following the ICH guideline Q2(R1). In order to check linearity, a calibration curve with six different BSA concentrations ranging between 50 and 500 µg/mL were measured as described above. The resulting calibration curve was linear and the corresponding correlation coefficient was 0.9998. All statistics of linear regression are summarized in Table 2. Furthermore, recovery experiments were performed at low (75 µg/mL), medium (250 µg/mL), and high (450 µg/mL) BSA concentrations in order to evaluate accuracy and precision. Therefore, protein concentration of the samples containing either BSA or BSA in combination with hydrolyzed PLGA-PEG-NP was determined in triplicate. Recovery data for BSA and the 95% confidence interval were shown in Table 3. Regardless of whether the sample contained hydrolyzed PLGA-PEG-NP, the protein recovery was between 91.4 and 99.5% for all examined concentration levels. Additionally, the small standard deviation confirmed the precision of the assay.

Quantification of total adsorbed protein amount for the different NP systems is displayed in Fig. 3. The measured serum protein amount for PLGA-100-NP was 99.1 µg/0.08 m^2 particle surface. The amount for PLGA-200-NP increased slightly to 104.0 µg/0.08 m^2 showing no significant change ($p \geq 0.05$). PEGylation of 100 and 200 nm PLGA-NP led to a significant decrease in protein adsorption ($p \leq 0.05$). The determined amount for PLGA-PEG-100-NP was 13.0 µg/0.08 m^2 and the amount for PLGA-PEG-200-NP remained almost the same ($p \geq 0.05$).

3.2.3. Protein identification by LC–MS/MS

The proteins bound onto the surface of 100 and 200 nm PLGA and PLGA-PEG-NP were identified after desorption and tryptic in-solution digestion using LC–MS/MS and subsequent bioinformatic interpretation of peptide fragmentation data.

We were able to detect numerous individual proteins in the corona of the different NP systems. Each sample was analyzed in three independent replicates. All identified proteins including their biological function in blood, molecular weight (M_W) as well as their calculated isoelectric point (pI) were listed in Table 4.

A total number of 29–39 different proteins was found in the corona of 100 and 200 nm PLGA-NP (Fig. 4). An exception was RUN 1 for the corona of PLGA-200-NP. Here, only 22 proteins were identified (Fig. 4B). The qualitative analysis of the proteins with respect to function, M_W, and pI showed that the corona of the two different sized PLGA-NP systems was almost comparable (Table 4, Figs. 4–6). Most of the proteins bound on the NP were related to specific functions in blood (Fig. 4) and displaying a pI > 5 (Fig. 6). The majority was constituted of proteins which are involved in the immune response, such as complement factor D, H, I, complement component 3, and C-C motif chemokine. Moreover, various apolipoproteins were identified, e.g. apolipoproteins A-I, A-II, and E (Fig. 4, Table 4).

In contrast, the quantitative as well as qualitative composition of proteins adsorbed onto the surface of PLGA-PEG-NP was considerably different (Table 4, Fig. 4). In total, the number of adsorbed proteins was lower and ranged between 16 and 23 with exception of RUN 3 for PLGA-PEG-200-NP (Fig. 4B, 29 proteins). Furthermore, the number of proteins involved in immune response was substantially lower. Corona proteins, such as complement factor D, I, and complement component 3 were depleted. The occurrence of apolipoproteins remained constant. In the corona of PLGA-PEG-100-NP even two additional apolipoproteins could be detected (C-III and IV). Besides, the proteins involved in the regulation of insulin-like growth factor (IGF) as well as other proteins i.e. gelsolin and beta-2-glycoprotein I disappeared completely in the corona of the PLGA-PEG-NP (Table 4, Fig. 4). The change in protein composition with PEGylation was also confirmed by dividing the proteins according to their M_W (Fig. 5). For PLGA-NP, the highest percentage of identified proteins was displayed by proteins with an average mass < 29 kDa, followed by proteins with an average mass from 66 to 118 kDa. This distribution was equal for PLGA-PEG-NP, but PEGylation led to a significant reduction of corona proteins with a mass above 118 kDa (Fig. 5).

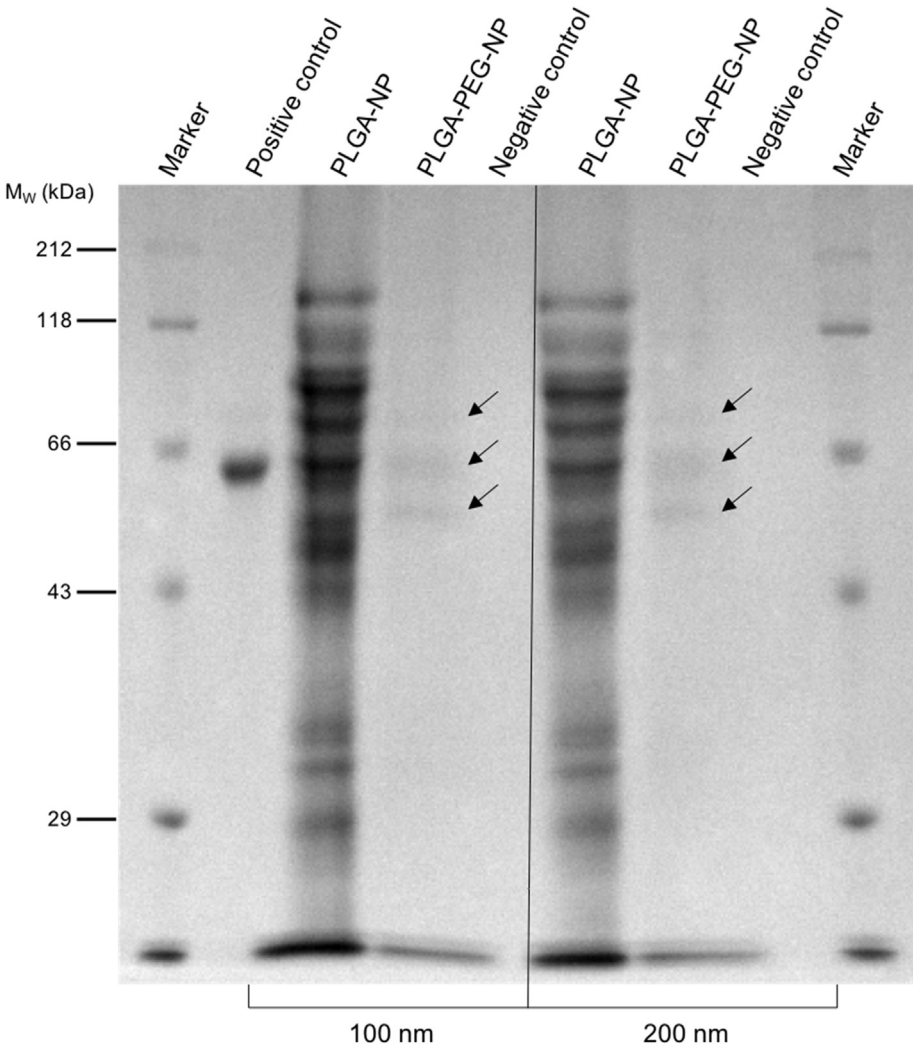

Fig. 2. One-dimensional SDS-PAGE gel of adsorbed serum proteins obtained from the corona of 100 and 200 nm PLGA- and PLGA-PEG-NP after 30 min incubation with FBS and subsequently washing. Negative controls derived from PLGA-PEG-NP (incubation without serum) and numbers on the left depict the molecular weight M_W (kDa) of marker proteins. The arrows mark the faintly visible protein bands from PLGA-PEG-NP.

Table 2
Statistics of linear regression for spectrophotometric quantification of BSA by Bradford protein assay.

Parameter	Spectrophotometric calibration for BSA
Slope b	1.2305 mL/mg
Standard Error S_b	0.0132 mL/mg
Intercept a	0.0259
Standard Error S_a	0.0040
Standard error of estimate $S_{y,x}$	0.0052
Correlation coefficient r	0.9998
Number of samples	6

4. Discussion

4.1. Corona protein quantification and NP size effects

The thoroughly characterization of manufactured NP is a prerequisite for further investigations of the protein corona and the following evaluation of size effects. The previously described solvent displacement and emulsion diffusion methods were suitable top-down preparations techniques for the reproducible production of PLGA- and PLGA-PEG-NP with a diameter of 100 and 200 nm, respectively [16,17]. A zeta potential absolute value of 30 mV is usually considered necessary for an solely electrostatic stabilization of particle colloids whereas in case of additional sterical stabilization a reduced zeta potential will be sufficient [21]. Hence, the zeta potential of about −40 mV for the different particle systems indicated colloidal stability due to electrostatic particle repulsion. Because of sufficient electrostatic stabilization and a monodisperse size distribution (PDI < 0.01), it can be assumed that the particles were not aggregated before incubation with FBS. Non-aggregated, single NP and a narrow size distribution are essential for elucidation of effects which just contribute to different sizes. AFM images confirmed the spherical shape and the smoothness of the particle surface (Fig. 1). A rough surface with local protrusions and depressions could alter the available surface and thus lead to a higher serum protein adsorption. For instance, Garcia-Alvarez et al. showed that gold nanostars adsorb significant larger amounts of proteins after *in vivo* injection into CD-1 mice due to their higher surface than gold nanorods [22]. Therefore, we referred in our experimental setup to a well-defined constant ratio of particle surface area to serum concentration.

In addition to the semi-quantitative analysis of adsorbed proteins by SDS-PAGE, Bradford protein assay was applied as a quantitative colorimetric approach to determine total NP bound protein amount and thereby achieving more detailed insights about the protein adsorption behavior. In previous studies bicinchoninic acid assay (BCA) was commonly used for quantification of corona proteins [23,24]. In 2005,

Table 3
Recovery data for the quantification of BSA using Bradford protein assay.

Parameter	BSA Level			BSA + hydrolyzed PLGA-PEG-NP Level		
	Low (75 µg/mL)	Medium (250 µg/mL)	High (450 µg/mL)	Low (75 µg/mL)	Medium (250 µg/mL)	High (450 µg/mL)
Recovery [%]	91.42	96.69	95.45	93.23	96.79	99.50
S.D. [%]	4.00	1.48	1.19	1.84	0.46	1.61
Confidence interval (p = 95%)						
Upper limit [%]	101.36	100.36	98.40	97.81	97.94	99.50
Lower limit [%]	81.49	93.02	92.49	88.66	95.64	91.52
Maximum [%]	96.01	97.66	96.82	94.94	97.16	97.00
Minimum [%]	88.65	94.99	94.73	91.29	96.27	93.81
Number of samples	3	3	3	3	3	3

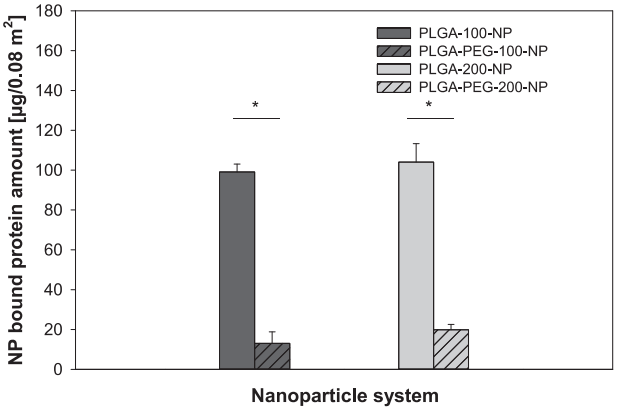

Fig. 3. Total serum protein amount bound onto the surface of the various NP systems. The differences in the mean values between PEGylated and non-PEGylated nanoparticles for both sizes were statistically significant (mean ± SD; n ≥ 3; $^{*}p \leq 0.05$).

Göppert and colleagues were the first who adapted this quantification method to NP [25]. However, we preferred Bradford protein assay because of its fast color development, the low variability of the staining between the different proteins in complex mixtures, and the minimal pipetting effort [18,26]. Nevertheless, it is well known in literature that chemicals, such as sodium dodecylsulfate (SDS), cause a modified response to the dye and thus lead to an altered absorbance of the sample [27]. Unfortunately, desorption of corona proteins with SDS from the NP surface is a widespread standard procedure before starting with protein analysis [28]. To overcome this fact, we established a new approach for NP-protein analysis. We hydrolyzed the NP-protein complexes with sodium hydroxide prior to addition of Bradford reagent. In order to evaluate potential interferences between the hydrolyzed NP compounds (e.g. lactic acid, PVA) and the protein-dye complex, we performed a method validation according to the ICH guideline Q2(R1). It could be shown, that the differences between the recovery of samples comprised of BSA or BSA plus hydrolyzed PLGA-PEG-NP were not significant at the three concentration levels used. Furthermore, with the small standard deviation the Bradford protein assay could be considered as an appropriate and reliable method for quantification of total bound protein amount of PLGA based NP systems within the examined concentration range.

One of the major goals of the present study was the investigation of the NP size impact on the formation of the protein corona. In the past several studies were conducted in order to investigate the protein adsorption on PLGA-NP [3,29,30]. However, a comparative examination of different sized PLGA-NP is still missing.

In Fig. 2 the protein pattern of the FBS positive control is illustrated, that was dominated by serum albumin which is the most abundant protein in blood [31]. On the other hand it is well known that protein adsorption on NP lead to a highly selective enrichment of proteins which exhibit a low abundance in blood [3]. Furthermore, Tenzer et al. showed, that binding profiles of these proteins not just correspond to the relative protein concentrations detected in plasma preparations [32]. In contrast to exhibiting only one band or protein, the PLGA-NP tend to adsorb numerous proteins on their surface displaying various functions in blood. This is in accordance with former reports, which revealed that protein adsorption is even more distinct on charged NP composed of hydrophobic core materials [4,33] and the negative surface charge enhances the adsorption of proteins with pI > 5.5 [3,34]. Our results suggested that the affinity of the serum proteins to both NP sizes is roughly the same.

In the case of spherical systems particle size is directly associated with the surface curvature. A reduction of size increases the ratio of total surface area to volume and therefore the free energy. Therefore, it is readily conceivable that many groups already observed a size-dependent effect on NP protein adsorption [7,35]. Schaeffler et al. showed that a reduction in gold NP (AuNP) size from 80 to 5 nm increases the protein binding capacity [36]. Dutta and collaborates demonstrated the same observation for amorphous silica NP (50–1000 nm) [37]. We hypothesize that the size difference between 100 and 200 nm is not large enough to significantly affect protein adsorption. Moreover, when NP are smaller than the average size of proteins, they are not able to develop a complete protein corona [38] while the structure and function of the proteins is retained upon adsorption [34]. Conversely, when NP diameter increases up to a threshold of 80 nm, adsorbed proteins undergo conformational changes which lead to further protein adsorption. A multilayer corona composed of 2–3 protein layers develops and the thickness of the corona increases [38]. Taking into account the above-mentioned limit, it is not surprising that there is no considerable difference in protein adsorption behavior between 100 and 200 nm PLGA-NP.

Concerning protein adsorption a reasonable comparison between PLGA-NP and 50 and 100 nm carboxyl-modified polystyrene NP can be drawn [28,39]. Both systems are composed of a polymeric core material and display a similar zeta potential of about −40 mV due to the terminal carboxyl groups. In addition, in previous studies with polystyrene NP the ratio of particle surface area to plasma concentration was also normalized in order to contemplate size effects. In contrast to our results, Lundqvist et al. detected only 50% homology between the coronas [39] and Zhang et al. showed significant protein abundance changes, too [28]. For instance, a significant smaller amount of haptoglobin related protein was bound to the 100 nm polystyrene NP [28]. Considering the aforementioned size limit of 80 nm and the different basic structure due to the aromatic hydrogen units, the difference to our results are not unexpected despite the similarities described. For this reason, size effects seem to be strongly dependent on the NP starting material.

In a further study a comparable qualitative protein pattern between 200 and 400 nm Fe_3O_4 NP was observed [40], whereas the amount of

Table 4
Identified proteins on the surface of 100 and 200 nm PLGA- and PLGA-PEG-NP. Proteins were identified in one (✓), two (✓✓) or three (✓✓✓) independent measurements by LC–MS/MS and subsequent data evaluation. Proteins were listed in alphabetical order. Molecular weight (M_W) and functions are taken from the web page https://www.uniprot.org/ and the isoelectric point (pI) was calculated by https://web.expasy.org/compute_pi/. Functions were categorized as blood coagulation (BC); Regulation of insulin-like growth factor (IGF); Immune response (IR); Lipoproteins (LP); Other serum components (OC); Oxygen transport (OT).

					Nanoparticle system			
					100 nm		200 nm	
Accession number	Protein	Function	M_W [Da]	pI	PLGA	PLGA-PEG	PLGA	PLGA-PEG
Q5E9B5	Actin, gamma-enteric smooth muscle	OC	41,877	5.31		✓✓		✓✓
B0JYQ0	ALB protein	OC	69,294	5.95	✓✓✓	✓✓	✓✓✓	✓✓✓
P34955	Alpha-1-antiproteinase	OC	46,104	6.05	✓	✓	✓	✓✓
B0JYN6	Alpha-2-HS-glycoprotein	OC	38,419	5.26		✓		✓✓✓
F1MSZ6	Antithrombin-III	BC	52,440	6.38		✓✓✓		✓
V6F9A2	Apolipoprotein A-I preproprotein	LP	30,276	5.71	✓✓✓	✓✓✓	✓✓✓	✓✓✓
P81644	Apolipoprotein A-II	LP	11,202	7.80	✓✓✓	✓✓✓	✓✓✓	✓✓✓
P19034	Apolipoprotein C-II	LP	11,061	5.67		✓✓	✓✓	✓✓✓
P19035	Apolipoprotein C-III	LP	10,692	5.02		✓		
Q3SYR5	Apolipoprotein C-IV	LP	14,438	8.75		✓		
Q0ZCB4	Apolipoprotein E	LP	27,074	8.87	✓✓✓	✓✓✓	✓✓✓	✓✓✓
P17690	Beta-2-glycoprotein 1	LP	38,252	8.53	✓✓✓		✓✓✓	
Q3ZC09	Beta-enolase	OC	47,096	7.60				✓
Q32L58	C-C motif chemokine	IR	10,337	8.43	✓✓✓		✓✓✓	
Q29RR9	C-C motif chemokine ligand 14	IR	10,457	8.98			✓	
F1N0I3	Coagulation factor V	BC	222,214	5.52	✓	✓✓	✓✓	
Q2TBQ1	Coagulation factor XIII B chain	BC	75,167	6.34	✓	✓	✓✓	
A8E654	COL18A1 protein	OC	135,068	5.60	✓			
P02453	Collagen alpha-1(I) chain	OC	138,939	5.60	✓✓			✓
P01030	Complement C4	IR	101,908	6.15	✓✓✓	✓✓✓	✓✓✓	✓✓✓
A0A0F6QNP7	Complement component 3	IR	187,181	6.46	✓✓✓		✓✓✓	✓
Q3T0A3	Complement factor D	IR	27,878	7.64	✓✓✓		✓✓✓	
Q28085	Complement factor H	IR	140,374	6.43	✓✓✓		✓✓✓	✓
F1MC45	Complement factor H precursor	IR	96,593	5.98	✓✓✓		✓	
Q32PI4	Complement factor I	IR	68,933	8.07	✓✓✓		✓✓✓	
Q17QC8	Complement factor properdin	IR	50,750	8.32	✓✓✓✓	✓	✓✓✓	✓
P01035	Cystatin-C	OC	16,265	9.23	✓✓✓	✓✓✓	✓✓✓	✓✓✓
A6QPP9	C-X-C motif chemokine	IR	12,609	9.30	✓✓✓		✓✓✓	✓
A5PJT7	ECM1 protein	IR	57,637	7.22	✓✓			
F1MYN5	Fibulin-1	OC	77,486	4.94	✓		✓✓	
F1N1I6	Gelsolin	CC	85,687	5.86	✓✓✓		✓✓✓	✓
P10096	Glyceraldehyde-3-phosphate dehydrogenase	OC	35,868	8.51		✓		✓✓
D4QBB3	Hemoglobin beta	OT	15,979	6.36		✓		✓
P02081	Hemoglobin fetal subunit beta	OT	15,859	6.51	✓✓✓	✓✓✓	✓✓✓	✓✓✓
P01966	Hemoglobin subunit alpha	OT	15,184	8.07	✓✓✓	✓✓✓	✓✓✓	✓✓✓
P02070	Hemoglobin subunit beta	OT	15,954	7.02		✓✓✓	✓	
Q1RMN8	Immunoglobulin light chain, lambda gene cluster	IR	24,536	7.54	✓			
Q2F6J3	Insulin-like growth factor 2 preproprotein	IGF	10,782	7.48	✓		✓✓	
P13384	Insulin-like growth factor-binding protein 2	IGF	34,015	7.13	✓✓✓		✓✓✓	
Q05716	Insulin-like growth factor-binding protein 4	IGF	27,890	7.10	✓✓		✓✓	
F1MUK3	Insulin-like growth factor-binding protein 6	IGF	24,953	8.73	✓✓		✓✓	
P01045	Kinogen-2	OC	68,710	6.09	✓			
P68301	Metallothionein-2	OC	6,028	8.23	✓✓			
Q8SPP7	Peptidoglycan recognition protein 1	OC	21,063	9.59	✓			
D1Z308	Periostin	OC	93,194	7.02		✓		✓
Q95121	Pigment epithelium-derived factor	OC	46,229	6,57	✓✓✓	✓	✓✓✓	✓
P06868	Plasminogen	BC	91,216	7.68				✓
Q2HJB6	Procollagen C-endopeptidase enhancer	OC	48,211	8.13	✓			
P00735	Prothrombin	BC	70,506	5.97	✓✓✓	✓✓✓	✓✓✓	✓✓
P82943	Regakine-1	IR	10,281	8.80	✓✓	✓✓	✓✓	
P02769	Serum albumin	OC	69,294	5.82	✓	✓✓✓		✓✓✓
P04815	Spleen trypsin inhibitor I	OC	10,843	9.00	✓✓	✓	✓✓	✓✓✓
Q2KIS7	Tetranectin	OC	22,144	5.47	✓✓✓	✓	✓✓	✓
Q28194	Thrombospondin-1	OC	25,015	7.94	✓	✓	✓✓	✓
E1BH06	Uncharacterized protein	IR	192,764	7.20	✓✓✓		✓✓✓	
F1MLW7	Uncharacterized protein	OC	24,397	7.53	✓		✓	
F1MVK1	Uncharacterized protein	OC	173,973	6.47	✓			✓
G3N0S9	Uncharacterized protein	OC	22,336	7.45	✓			
Q3ZBS7	Vitronectin	CC	53,575	5.92			✓	

protein adsorption differed between both systems which was detected by relative quantification by LC–MS/MS. This quantification method allows one to reliably detect even minimal size dependent differences in protein adsorption affinities which cannot be detected by spectrophotometric determination of total adsorbed protein amount by Bradford protein assay. In consequence, the heterogenous data situation regarding the effect of size on protein corona formation could also result from the analytical limitations of the methods used.

The above explained arguments regarding the size are not only appropriate for PLGA-NP but also for PLGA-PEG-NP of both sizes.

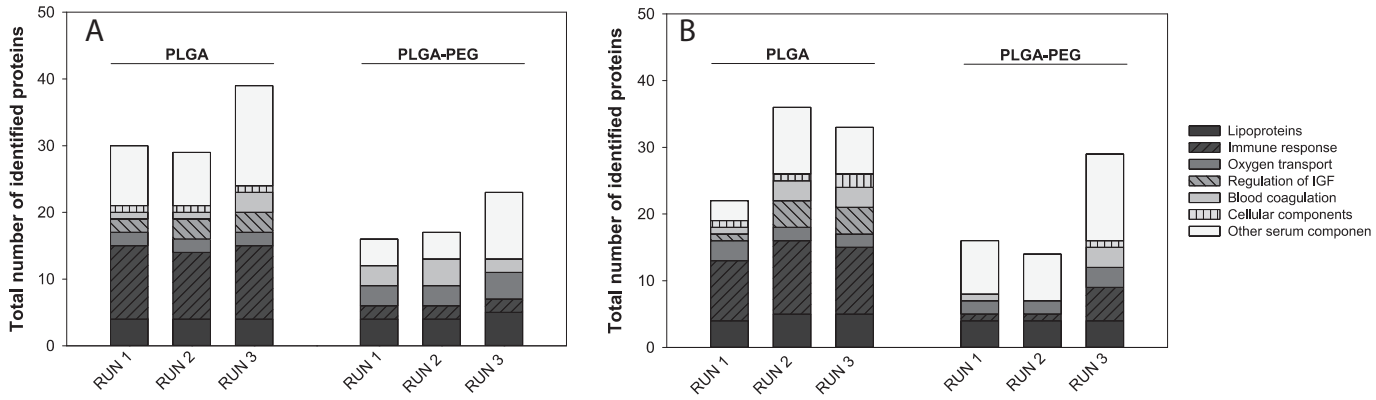

Fig. 4. Total number of identified proteins in the corona of (A) 100 nm PLGA- and PLGA-PEG-NP, (B) 200 nm PLGA- and PLGA-PEG-NP. Proteins were analyzed by LC–MS/MS in three independent measurements (RUN 1–3) and grouped according to their function in blood. IGF = insulin-like growth factor.

However, the differing adsorption profiles of PLGA-PEG-NP in comparison to PLGA-NP will be discussed subsequently.

4.2. Effect of PEGylation on the formation of the protein corona

Coating the surface of nanocarriers with PEG is a widespread strategy to prolong their systemic circulation time and therefore enhance the ability to reach the desired target cell [9]. Gref and collaborates established the first PEGylated polymeric nanospheres [41]. They demonstrated that PEGylation of PLGA-NP increases blood circulation time after injection into mice while reducing liver uptake in comparison to their non-PEGylated counterparts. In order to evaluate 'stealth' properties, we prepared NP using an amphiphile diblock copolymer consisting of D,L-lactide and glycolide in equal parts covalently attached to a PEG entity (5 kDa). During preparation process, the PEG chains migrate from the emulsification droplets to the water interface while the hydrophobic residue remained into the inner core resulting in a PEG surface coating after organic solvent evaporation and NP precipitation [41]. For this reason, we assumed the PEG surface density as 15 wt% [16].

Our results indicated that PLGA-PEG-NP led to a significant reduced amount of bound serum proteins and a considerable distinct protein profile compared to PLGA-NP (Figs. 2 and 3). Due to the hydrophilic characteristics of the PEG chains, the NP surface is covered by a hydrated PEG layer exhibiting a large extended volume. When proteins approach the surface, the flexible PEG chains become compressed which creates an unfavorable thermodynamically situation. Consequently, PEGylation prevents NP against opsonization resulting in a lower immunogenicity [9,30]. The shielding effect substantially depends on the PEG chain length and PEG surface density. In general, a M_W of 2 kDa is considered as sufficient for reducing recognition by immune cells [9]. According to Gref et al., no further decrease in protein adsorption can be observed above a PEG M_W of 5 kDa. Furthermore, a PEG density of 5 wt% is determined as the threshold for maximum protein adsorption reduction [30]. Taking into account the above-mentioned limits and the characteristics of our PEGylated NP systems, the drastically suppression of protein adsorption was readily conceivable. Nevertheless, it is not possible to inhibit protein adsorption entirely [22,24,30]. In a recent pioneering study, Schöttler and coworkers demonstrated that not only the reduced amount of opsonizing proteins is the driving force for 'stealth' properties but also a selective enrichment of certain proteins is required. They identified clusterin, also known as apolipoprotein J, as a new dysopsonin [42]. Instead of clusterin, we identified serum albumin, another protein with dysopsonic properties, on the surface of all investigated NP systems [40]. Thus Ogawara and colleagues revealed that blood circulation of human serum albumin pre-coated polystyrene NP is prolonged after injection into rats compared to the pristine NP [43]. According to the highlighted protein band at a M_W of 67 kDa (Fig. 2), we suggested an enrichment of serum albumin in the corona of the PLGA-PEG-NP and therefore also assuming an increased blood circulation lifetime.

We identified a large number of proteins in the corona of the non-PEGylated NP displaying various physiological functions (Fig. 3, Table 4). Even though serum is composed of about 3700 different proteins, the majority of corona constituents generally take part in immune response, lipid transport, blood coagulation or iron transport [44]. The corona of the PEGylated NP was less complex and the appearance of higher molecular weight proteins was partially repressed

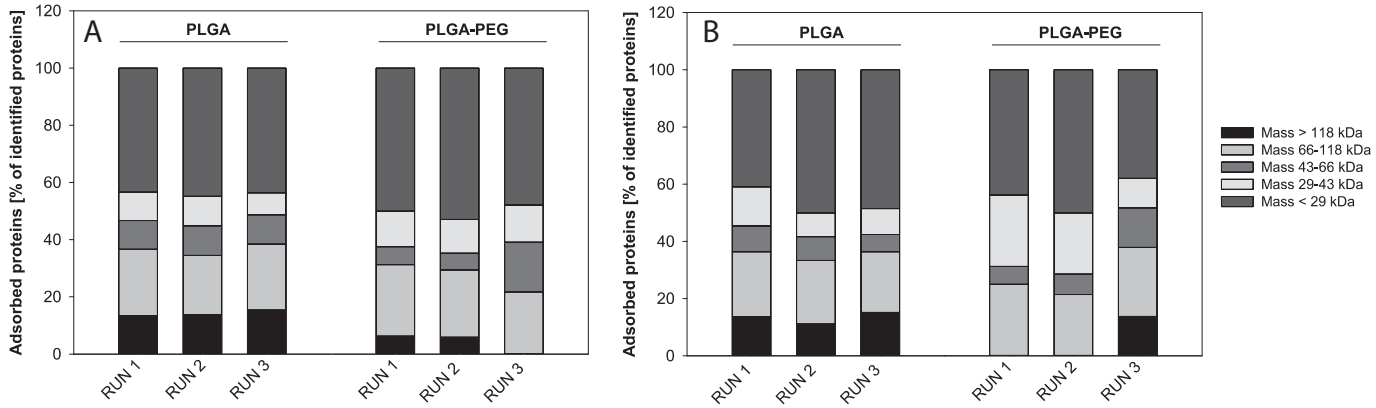

Fig. 5. Classification of corona proteins according to their molecular mass for (A) 100 nm PLGA- and PLGA-PEG-NP and (B) 200 nm PLGA- and PLGA-PEG-NP. Proteins were identified in three independent measurements by LC–MS/MS (RUN 1–3) and the molecular mass was taken from the web page https://www.uniprot.org/.

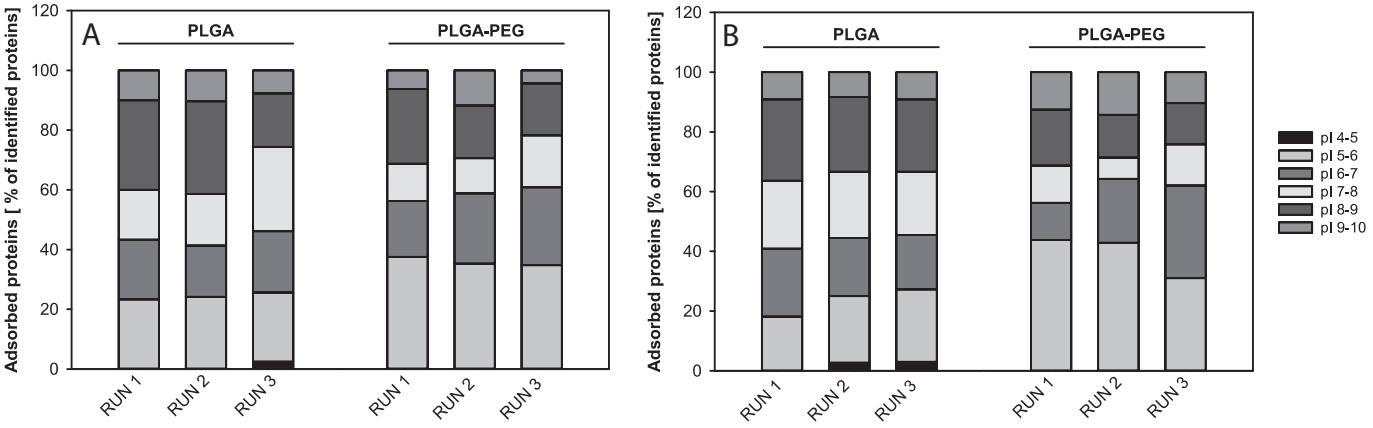

Fig. 6. Classification of corona proteins according to their isoelectric point (pI) for (A) 100 nm PLGA- and PLGA-PEG-NP and (B) 200 nm PLGA- and PLGA-PEG-NP. Proteins were identified in three independent measurements by LC–MS/MS (RUN 1–3) and the isoelectric point was calculated by https://web.expasy.org/compute_pi/.

which is consistent with previous observations [24]. However, the most striking observation was the decreased number of proteins involved into immunoregulatory processes. These proteins are known to be opsonins. After adsorption they facilitate phagocytosis by cells of the MPS via opsonin-recognizing receptors, for example complement and Fc receptors [9,10]. The adsorption of opsonins is primarily mediated by hydrophobic interactions [45]. PEGylation led to a more hydrophilic surface and therefore adsorption of opsonins declined. For instance, Walkey and coworkers reported that the amount of complement factor C3 decreased from 30 to 5% w/w of total adsorbed protein when gold NP were grafted with PEG [24]. In case of PLGA-PEG-NP complement compound 3 vanished completely. In a current study Chen et al. emphasized the role of the complement system in blood clearance mechanisms of nanospheres [46]. The complement system is part of the innate immune system which eliminates infectious microbes. Besides, C3 is a critical key factor in the three separated pathways (classical, lectin and alternative) of the activation cascade [47]. They investigated uptake into human leukocytes after incubation of SPIO nanoworms with either human plasma or plasma with blocked complement opsonization by adding 10 mM EDTA. Results showed that uptake is significantly reduced when complement system is inhibited [46]. Nonetheless, one has to keep in mind that complement activation is probably not the sole mechanism of elimination [48].

Apolipoproteins are involved in lipid trafficking and were detected to be enriched on the surface of various different nanocarriers [44]. In general, they exhibit dysopsonic properties [3]. Moreover, coating NP with polysorbate 80 leads to a preferential adsorption of apolipoprotein E which enables the transport across the blood-brain barrier [49]. The same phenomenon was observed after covalent attachment of apolipoprotein A-I to human serum albumin NP [50]. After FBS incubation both proteins were identified in the corona of PLGA and PLGA-PEG-NP underlining the involvement in cell transport mechanisms and biodistribution. Beta-2-glycoprotein I is structurally associated with the lipoproteins and is therefore also referred to as apolipoprotein H. In contrast to the other identified apolipoproteins it is assigned to the class of opsonins. The rapid clearance rate of anionic liposomes in mice is correlated to the amount of bound beta-2-glycoprotein I. Besides, pretreating the animals with anti-human beta-2-glycoprotein I antibodies prolonged significantly the circulation time [51]. Interestingly, beta-2-glycoprotein I was determined in three independent measurements by LC–MS/MS in the corona of 100 and 200 nm PLGA-NP, whereas it could not be found a single time in the corona of the PLGA-PEG-NP (Table 4). This fact leads to the assumption that the produced PLGA-PEG-NP of both sizes will represent a favorable body distribution profile with the ability of an extended blood circulation lifetime.

5. Conclusion

In the present study, we demonstrated that Bradford protein assay represents a suitable approach for quantification of total adsorbed protein amount after alkaline hydrolysis of PLGA based NP systems. It provides reliable results within the examined concentration range and therefore allowing a more in-deep understanding of protein corona formation after FBS incubation. One objective was to investigate the effect of NP size on protein adsorption. The data situation on this topic is very heterogeneous and no clear tendency becomes apparent regardless of the NP starting material. In many cases it is difficult to separate the effect of size from other influential factors on the corona formation. Additionally, variations in analytical methods can make directly comparisons of individual studies challenging. Here, the ratio of total particle surface area to serum concentration was kept constant for the different particle systems in order to solely investigate the impact of size. Consequently, it can be stated that protein adsorption did not depend on the size of PLGA- and PLGA-PEG-NP within the range of 100 and 200 nm. A lot of different proteins with varying functions in body were identified in the corona of PLGA-NP indicating that they are prone to opsonization. PEGylation led to a significant lower amount of bound proteins and a less complex protein pattern. Taking into account the suppression of proteins which are involved into immune response, the proposed PEGylated NP are representing excellent long-circulating drug carrier systems with the unique opportunity to potentially take advantage of enhanced permeability and retention effect (EPR).

References

[1] A. Nel, T. Xia, L. Mädler, N. Li, Toxic potential of materials at the nanolevel, Science 311 (2006) 622–627.
[2] J. Klein, Probing the interactions of proteins and nanoparticles, Proc. Natl. Acad. Sci. USA 104 (2007) 2029–2030.
[3] R. Gossmann, E. Fahrländer, M. Hummel, D. Mulac, J. Brockmeyer, K. Langer, Comparative examination of adsorption of serum proteins on HSA- and PLGA-based nanoparticles using SDS-PAGE and LC-MS, Eur. J. Pharm. Biopharm. 93 (2015) 80–87.
[4] T. Cedervall, I. Lynch, S. Lindmann, T. Berggard, E. Thulin, H. Nilsson, K.A. Dawson, Understanding the nanoparticle-protein corona using methods to quantify exchange rates and affinities of protein for nanoparticles, Proc. Natl. Acad. Sci. USA 104 (2007) 2050–2055.
[5] L. Vroman, A.L. Adams, G.C. Fischer, P.C. Munoz, Interaction of high molecular weight kininogen, factor XII, and fibrinogen in plasma at interfaces, Blood 55 (1990) 156–159.
[6] D. Docter, D. Westmeier, M. Markiewicz, S. Stolte, S.K. Knauer, R.H. Stauber, The nanoparticle biomolecule corona: lessons learned - challenge accepted? Chem. Soc. Rev. 44 (2015) 6094–6121.
[7] V.H. Nguyen, B.J. Lee, Protein corona: a new approach for nanomedicine design, Int. J. Nanomed. 12 (2017) 3137–3151.
[8] F. Danhier, E. Ansorena, J.M. Silva, R. Coco, A. Le Breton, V. Preat, PLGA-based nanoparticles: an overview of biomedical applications, J. Control. Release 161

(2012) 505–522.
[9] D.E. Owens 3rd, N.A. Peppas, Opsonization, biodistribution, and pharmacokinetics of polymeric nanoparticles, Int. J. Pharm. 307 (2006) 93–102.
[10] J.S. Suk, Q. Xu, N. Kim, J. Hanes, L.M. Ensign, PEGylation as a strategy for improving nanoparticle-based drug and gene delivery, Adv. Drug Deliv. Rev. 99 (2016) 28–51.
[11] E. Calzoni, A. Cesaretti, A. Polchi, A. Di Michele, B. Tancini, C. Emiliani, Biocompatible polymer nanoparticles for drug delivery applications in cancer and neurodegenerative disorder therapies, J. Funct. Biomater. 10 (2019) 1–15.
[12] C. Pisani, E. Rascol, C. Dorandeu, J.C. Gaillard, C. Charnay, Y. Guari, J. Chopineau, J. Armengaud, J.M. Devoisselle, O. Prat, The species origin of the serum in the culture medium influences the in vitro toxicity of silica nanoparticles to HepG2 cells, PLoS One 12 (2017) e0182906.
[13] C. Gräfe, A. Weidner, M.V. Luhe, C. Bergemann, F.H. Schacher, J.H. Clement, S. Dutz, Intentional formation of a protein corona on nanoparticles: serum concentration affects protein corona mass, surface charge, and nanoparticle-cell interaction, Int. J. Biochem. Cell Biol. 75 (2016) 196–202.
[14] M.P. Monopoli, D. Walczyk, A. Campbell, G. Elia, I. Lynch, F.B. Bombelli, K.A. Dawson, Physical-chemical aspects of protein corona: relevance to in vitro and in vivo biological impacts of nanoparticles, J. Am. Chem. Soc. 133 (2011) 2525–2534.
[15] C.E. Astete, C.M. Sabliov, Synthesis and characterization of PLGA nanoparticles, J. Biomater. Sci. Polym. Ed. 17 (2006) 247–289.
[16] S. Spek, M. Häuser, M.M. Schäfer, K. Langer, Characterisation of PEGylated PLGA nanoparticles comparing the nanoparticle bulk to the particle surface using UV/vis spectroscopy, SEC, 1H NMR spectroscopy, and X-ray photoelectron spectroscopy, Appl. Surf. Sci. 347 (2015) 378–385.
[17] J. Anderski, L. Mahlert, D. Mulac, K. Langer, Mucus-penetrating nanoparticles: promising drug delivery systems for the photodynamic therapy of intestinal cancer, Eur. J. Pharm. Biopharm. 129 (2018) 1–9.
[18] M.M. Bradford, A rapid and sensitive method for the quantitation of microgram quantities of protein utilizing the principle of protein-dye binding, Anal. Biochem. 72 (1976) 248–254.
[19] J. Zhang, L. Xin, B. Shan, W. Chen, M. Xie, D. Yuen, W. Zhang, Z. Zhang, G.A. Lajoie, B. Ma, PEAKS DB: de novo sequencing assisted database search for sensitive and accurate peptide identification, Mol. Cell. Proteom. 11 (2012) M111.010587-010581–M010111.010587-010588.
[20] B. Ma, K. Zhang, C. Hendrie, C. Liang, M. Li, A. Doherty-Kirby, G. Lajoie, PEAKS: powerful software for peptide de novo sequencing by tandem mass spectrometry, Rapid Commun. Mass Spectrom. 17 (2003) 2337–2342.
[21] E. Casals, T. Pfaller, G.J. Oostingh, Puntes, V., Time evolution of the nanoparticle protein corona, ACS Nano 4 (2009) 3623–3632.
[22] R. Garcia-Alvarez, M. Hadjidemetriou, A. Sanchez-Iglesias, L.M. Liz-Marzan, K. Kostarelos, In vivo formation of protein corona on gold nanoparticles. The effect of their size and shape, Nanoscale 10 (2018) 1256–1264.
[23] V. Mirshafiee, R. Kim, S. Park, M. Mahmoudi, M.L. Kraft, Impact of protein precoating on the protein corona composition and nanoparticle cellular uptake, Biomaterials 75 (2016) 295–304.
[24] C.D. Walkey, J.B. Olsen, H. Guo, A. Emili, W.C. Chan, Nanoparticle size and surface chemistry determine serum protein adsorption and macrophage uptake, J. Am. Chem. Soc. 134 (2012) 2139–2147.
[25] T.M. Göppert, R.H. Müller, Protein adsorption patterns on poloxamer- and poloxamine-stabilized solid lipid nanoparticles (SLN), Eur. J. Pharm. Biopharm. 60 (2005) 361–372.
[26] S.M. Read, D.H. Northcote, Minimization of variation in the response to different proteins of the Coomassie Blue G dye-binding assay for protein, Anal. Biochem. 116 (1981) 53–64.
[27] C.M. Stoscheck, Increased uniformity in the response of the Coomassie Blue protein assay to different proteins, Analyt. Biochem. 184 (1990) 111–116.
[28] H. Zhang, K.E. Burnum, M.L. Luna, B.O. Petritis, J.S. Kim, W.J. Qian, R.J. Moore, A. Heredia-Langner, B.J. Webb-Robertson, B.D. Thrall, D.G. Camp 2nd, R.D. Smith, J.G. Pounds, T. Liu, Quantitative proteomics analysis of adsorbed plasma proteins classifies nanoparticles with different surface properties and size, Proteomics 11 (2011) 4569–4577.
[29] K. Sempf, T. Arrey, S. Gelperina, T. Schorge, B. Meyer, M. Karas, J. Kreuter, Adsorption of plasma proteins on uncoated PLGA nanoparticles, Eur. J. Pharm. Biopharm. 85 (2013) 53–60.
[30] R. Gref, M. Lück, P. Quellec, M. Marchand, E. Dellacherie, S. Harnisch, T. Blunk, R.H. Müller, 'Stealth' corona-core nanoparticles surface modified by polyethylene glycol (PEG): influences of the corona (PEG chain length and surface density) and of the core composition on phagocytic uptake and plasma protein adsorption, Colloids Surf. B Biointerfaces 18 (2000) 301–313.
[31] P.G. Righetti, A. Castagna, F. Antonucci, C. Piubelli, D. Cecconi, N. Campostrini, C. Rustichelli, P. Antonioli, G. Zanusso, S. Monaco, L. Lomas, E. Boschetti, Proteome analysis in the clinical chemistry laboratory: myth or reality? Clin. Chim. Acta 357 (2005) 123–139.
[32] T. Tenzer, D. Docter, S. Rosfa, A. Wlodarski, J. Kuharev, A. Rekik, S.K. Knauer, C. Bantz, T. Nawroth, C. Bier, J. Sirirattanapan, W. Mann, L. Treusel, R. Zellner, M. Maskos, H. Schild, R.H. Stauber, Nanoparticle size is a critical physico-chemical determinat of the human blood plasma corona: a comprehensive quantitative proteomic analysis, ASC Nano 5 (2011) 7155–7167.
[33] A. Gessner, A. Lieske, B.R. Paulke, R.H. Müller, Influence of surface charge density on protein adsorption on polymeric nanoparticles: analysis by two-dimensional electrophoresis, Eur. J. Pharm. Biopharm. 54 (2002) 165–170.
[34] P. Aggarwal, J.B. Hall, C.B. McLeland, M.A. Dobrovolskaia, S.E. McNeil, Nanoparticle interaction with plasma proteins as it relates to particle biodistribution, biocompatibility and therapeutic efficacy, Adv. Drug Deliv. Rev. 61 (2009) 428–437.
[35] D. Chen, S. Ganesh, W. Wang, M. Amiji, Plasma protein adsorption and biological identity of systeically administered nanoparticles, Int. J. Nanomed. 12 (2017) 2113–2135.
[36] M. Schaffler, M. Semmler-Behnke, H. Sarioglu, S. Takenaka, A. Wenk, C. Schleh, S.M. Hauck, B.D. Johnston, W.G. Kreyling, Serum protein identification and quantification of the corona of 5, 15 and 80 nm gold nanoparticles, Nanotechnology 24 (2013) 265103–265111.
[37] D. Dutta, S.K. Sundaram, J.G. Teeguarden, B.J. Riley, L.S. Fifield, J.M. Jacobs, S.R. Addleman, G.A. Kaysen, B.M. Moudgil, T.J. Weber, Adsorbed proteins influence the biological activity and molecular targeting of nanomaterials, Toxicol. Sci. 100 (2007) 303–315.
[38] J. Piella, N.G. Bastus, V. Puntes, Size-dependent protein-nanoparticle interactions in citrate-stabilized gold nanoparticles: the emergence of the protein corona, Bioconjug. Chem. 28 (2017) 88–97.
[39] M. Lundqvist, J. Stigler, G. Elia, I. Lynch, T. Cedervall, K.A. Dawson, Nanoparticle size and surface properties determine the protein corona with possible implications for biological impacts, Proc. Natl. Acad. Sci. USA 105 (2008) 14265–14270.
[40] Z. Hu, H. Zhang, Y. Zhang, R. Wu, H. Zou, Nanoparticle size matters in the formation of plasma protein coronas on Fe3O4 nanoparticles, Colloids Surf. B Biointerfaces 121 (2014) 354–361.
[41] R. Gref, Y. Minamitake, M.T. Peracchia, V. Trubetskoy, V. Torchilin, R. Langer, Biodegradable long-circulating polymeric nanospheres, Science 263 (1994) 1600–1603.
[42] S. Schöttler, G. Becker, S. Winzen, T. Steinbach, K. Mohr, K. Landfester, V. Mailander, F.R. Wurm, Protein adsorption is required for stealth effect of poly (ethylene glycol)- and poly(phosphoester)-coated nanocarriers, Nat. Nanotechnol. 11 (2016) 372–377.
[43] K. Ogawara, K. Furumoto, S. Nagayama, K. Minato, K. Higaki, T. Kai, T. Kimura, Pre-coating with serum albumin reduces receptor-mediated hepatic disposition of polystyrene nanosphere: implications for rational design of nanoparticles, J. Control. Release 100 (2004) 451–455.
[44] C.D. Walkey, W.C. Chan, Understanding and controlling the interaction of nanomaterials with proteins in a physiological environment, Chem. Soc. Rev. 41 (2012) 2780–2799.
[45] A. Gessner, R. Waicz, A. Lieske, B.R. Paulke, K. Mäder, R.H. Müller, Nanoparticles with decreasing surface hydrophobicities: influence on plasma protein adsorption, Int. J. Pharm. 196 (2000) 245–249.
[46] F. Chen, G. Wang, J.I. Griffin, B. Brenneman, N.K. Banda, V.M. Holers, D.S. Backos, L. Wu, S.M. Moghimi, D. Simberg, Complement proteins bind to nanoparticle protein corona and undergo dynamic exchange in vivo, Nat. Nanotechnol. 12 (2017) 387–393.
[47] D. Ricklin, G. Hajishengallis, K. Yang, J.D. Lambris, Complement: a key system for immune surveillance and homeostasis, Nat. Immunol. 11 (2010) 785–797.
[48] N. Bertrand, P. Grenier, M. Mahmoudi, E.M. Lima, E.A. Appel, F. Dormont, J.M. Lim, R. Karnik, R. Langer, O.C. Farokhzad, Mechanistic understanding of in vivo protein corona formation on polymeric nanoparticles and impact on pharmacokinetics, Nat. Commun. 8 (2017) 1–7.
[49] J. Kreuter, D. Shamenkov, V. Petrov, P. Ramge, K. Cychutek, C. Koch-Brandt, R. Alyautdin, Apolipoprotein-mediated transport of nanoparticle-bound drugs across the blood-brain barrier, J. Drug Target. 10 (2002) 317–325.
[50] J. Kreuter, T. Hekmatara, S. Dreis, T. Vogel, S. Gelperina, K. Langer, Covalent attachment of apolipoprotein A-I and apolipoprotein B-100 to albumin nanoparticles enables drug transport into the brain, J. Control. Release 118 (2007) 54–58.
[51] A. Chonn, S.C. Semple, R. Cullis, beta-2-Glycoprotein I is a major protein associated with very rapidly cleared liposomes in vivo, suggesting a significant role in the immune clearance of "non-self" particles, J. Biol. Chem. 270 (1995) 25845–25849.